Zoosyst. Evol. 100 (1) 2024, 167–182 | DOI 10.3897/zse.100.114016

PENSOFT

für Naturkunde MUSEUM FÜR NATURKUNDE BERLIN

Integrative description of a new species of *Dugesia* (Platyhelminthes, Tricladida, Dugesiidae) from southern China, with its complete mitogenome and a biogeographic evaluation

Ying Zhu[1], JiaJie Huang[1], Ronald Sluys[2], Yi Liu[1], Ting Sun[1], An-Tai Wang[1], Yu Zhang[1,3]

1 *Shenzhen Key Laboratory of Marine Bioresource and Eco-environmental Science, College of Life Science and Oceanography, Shenzhen University, Shenzhen, Guangdong, China*

2 *Naturalis Biodiversity Center, P.O. Box 9517, 2300 RA Leiden, Netherlands*

3 *Guangdong Engineering Research Center for Marine Algal Biotechnology, College of Life Sciences and Oceanography, Shenzhen University, Shenzhen, Guangdong, China*

https://zoobank.org/808B9FAB-975D-4A59-8D9F-18E7F4A176D3

Corresponding author: Yu Zhang (biozy@szu.edu.cn)

Academic editor: Pavel Stoev ♦ **Received** 13 October 2023 ♦ **Accepted** 10 January 2024 ♦ **Published** 16 February 2024

Abstract

A new species of freshwater flatworm of the genus *Dugesia* from Guangdong Province in China is described through an integrative approach, including molecular and morphological data, as well as mitochondrial genome analysis. The new species, *Dugesia ancoraria* Zhu & Wang, **sp. nov.**, is characterised by: (a) a highly asymmetrical penis papilla, provided with a hunchback-like dorsal bump; (b) a short duct between seminal vesicle and ejaculatory duct; and (c) a postero-ventral course of the ejaculatory duct, which opens to the exterior at the subterminal, ventral part of the penis papilla. The molecular phylogenetic tree obtained from the concatenated dataset of four DNA markers (18S rDNA, ITS-1, 28S rDNA, COI) facilitated determination of the phylogenetic position of the new species, which shares a sister-group relationship with a small clade, comprising *D. notogaea* Sluys & Kawakatsu, 1998 from Australia and *D. bengalensis* Kawakatsu, 1983 from India. The circular mitogenome of the new species is 17,705 bp in length, including 12 protein coding genes, two ribosomal genes, and 22 transfer RNAs. Via analysis of gene order of mitochondrial genomes, the presently available pattern of mitochondrial gene rearrangement in the suborder Continenticola is discussed.

Key Words

biogeography, *Dugesia*, mitogenome, molecular phylogeny, taxonomy

Introduction

The distributional range of freshwater planarians of the genus *Dugesia* Girard, 1850 covers a large part of the Old World and Australia (cf. Sluys and Riutort 2018, fig. 13B). The historical biogeography of the genus has attracted the attention of planarian specialists for already a good number of years (cf. Sluys et al. 1998 and references therein), culminating in the most recent analysis, which could make use of a time-calibrated phylogenetic tree (Solà et al. 2022).

From the approximately 110 known species of *Dugesia*, thus far only 12 species have been recorded from China, namely, *D. japonica* Ichikawa & Kawakatsu, 1964; *D. ryukyuensis* Kawakatsu, 1976; *D. sinensis* Chen & Wang, 2015; *D. umbonata* Song & Wang, 2020; *D. semiglobosa* Chen & Dong, 2021; *D. majuscula* Chen & Dong, 2021; *D. circumcisa* Chen & Dong, 2021; *D. verrucula* Chen & Dong, 2021; *D. constrictiva* Chen & Dong, 2021; *D. gemmulata* Sun & Wang, 2022; *D. aduncа* Chen & Sluys, 2022; and *D. tumida* Chen & Sluys, 2022. The present study adds a new species of *Dugesia* to

the Chinese fauna by describing it through an integrative approach, involving morphological, molecular phylogenetic and mitogenomic analyses. Among these methods, morphological characters, especially the anatomy of the copulatory apparatus, form the main source for the description and identification of the new species.

Since the mitogenome is characterized by strict gene homology and uniparental inheritance without recombination, and contains genes that evolve at different rates, mitochondrial gene order is considered as a strong genetic marker for resolving the phylogenetic position of new species (Rosa et al. 2017). Unfortunately, mitochondrial genomic information on freshwater planarians is still highly limited. Therefore, we expanded our taxonomic study by including also the sequencing and annotation of the complete mitogenome of the new species *Dugesia ancoraria* Zhu & Wang, sp. nov. and compare its gene order with that of other species in the suborder Continenticola Carranza et al., 1998 for which such information is currently available from GenBank.

Materials and methods

Sample collection and culturing

Specimens were collected from a narrow artificial canal running from Wenshan lake in Shenzhen city, Guangdong Province, China (22°31'55"N, 113°56'21"E) on 10 May 2021 (Fig. 1). A 200-µm-mesh sieve was used to collect *Cladophora* algae, to which the worms were attached. The contents of the mesh sieve were washed into a bucket using habitat water, and then transported to the laboratory of Shenzhen University for further analysis and culturing. The flatworms were reared in a glass aquarium (21 cm × 15 cm; depth 18 cm) at room temperature (23–26 °C). The culture was aerated, and the flatworms were fed daily with *Daphnia*.

DNA extraction, amplification, sequencing and phylogenetic analysis

After starvation for three days, total DNA was extracted from three sexual individuals using the E.Z.N.A.™ Mollusc DNA Isolation Kit (Omega, Norcross, GA, USA). Four gene fragments, namely 18S ribosomal gene (18S rDNA), 28S ribosomal gene (28S rDNA), ribosomal internal transcribed spacer-1 (ITS-1), and cytochrome C oxidase subunit I (COI), were amplified by polymerase chain reaction (PCR). We used 2×Taq Plus Master Mix II (Vazyme, China) to amplify 18S rDNA, 28S rDNA, ITS-1, and COI. Primers used for amplification and the PCR protocol are listed in Table 1. Forward and reverse DNA strands were determined by Sanger sequencing either at BGI (Guangzhou, China) or TsingKe Biotech (Beijing, China). All new sequences have been uploaded to GenBank, NCBI (Table 2).

To determine the phylogenetic position of the new species within the genus *Dugesia*, we generated datasets consisting of marker gene sequences (18S rDNA, 28S rDNA, ITS-1, and COI; see Table 2) of the new species *Dugesia ancoraria* and available sequences of other *Dugesia* species from GenBank, NCBI, as well as two outgroup species, viz., *Recurva postrema* Sluys & Solà, 2013 (ITS-1 sequence not available in GenBank, NCBI), and *Schmidtea mediterranea* (Benazzi, Baguñà, Ballester, Puccinelli & del Papa, 1975).

Nuclear ribosomal markers were aligned with MAFFT (online version 7: MAFFT alignment and NJ / UPGMA phylogeny (cbrc.jp), Katoh et al. 2017) using the E-INS-i algorithm, while mitochondrial coding gene COI was aligned by MASCE v2.03 (Ranwez et al. 2018). In order to check for the absence of stop codons, COI sequences were translated into amino acids by ORFFINDER in NCBI, applying genetic code 9 before alignment, after which regions of ambiguous alignments were removed by Gblocks v0.91b (Talavera and Castresana 2007), using the same parameters as specified in Li et al. (2019). For ribosomal DNA, sequences were excluded by ClipKIT (Steenwyk et al. 2020) with kpic-gappy mode to keep parsimony-informative and constant sites and to remove highly gappy sites. Final length of the alignments was 693 base pairs (bp) for COI, 1,388 bp for 18S rDNA, 1,383 bp for 28S rDNA, and 591 bp for ITS-1. To ensure sequences' validity, the substitution saturation test (Xia et al. 2003; Xia and Lemey 2009) in DAMBE6 software (Xia 2017) was used to evaluate the nucleotide substitution saturation of four datasets, followed by the assembly of a multi-gene concatenated dataset (with the order 18S rDNA–28S rDNA–ITS-1–COI), using SequenceMatrix v1.8 (Vaidya et al. 2011). Sequences that were shorter or not available in GenBank were completed with "-". We used PartitionFinder2 (Lanfear et al. 2017) to evaluate the best-fit evolution models by estimating independent models of molecular evolution for subsets of sites that were deemed to have evolved in similar ways.

Table 1. Primer sequences used for PCR amplification.

Gene	Primer	Sequence (5'-3')	Reference	PCR protocol
COI	COIEFMF	Forward: GGW GGK TTT GGW AAW TG		94 °C 5 min, 35× (94 °C 50 s,
	COIRSong	Reverse: GWG CAA CAA CAT ART AAG TAT CAT		50 °C 45 s, 72 °C 45 s); 72 °C 7 min
ITS-1	ITS9F	Forward: GTA GGT GAA CCT GCG GAA GG	Baguñà et al. 1999	98 °C 5 min, 30× (98 °C 30 s,
	ITSR	Reverse: TGC GTT CAA ATT GTC AAT GAT C		46 °C 45 s, 72 °C 30 s); 72 °C 7 min
18S rDNA	18S 1F	Forward: TAC CTG GTT GAT CCT GCC AGT AG	Carranza et al. 1996	94 °C 5 min, 40× (95 °C 50 s,
	18S 9R	Reverse: GAT CCT TCC GCA GGT TCA CCT AC		50 °C 45 s, 72 °C 50 s); 72 °C 7 min
28S rDNA	28S 1F	Forward: TAT CAG TAA GCG GAG GAA AAG	Álvarez-Presas et al. 2008	94 °C 5 min, 40× (94 °C 50 s,
	28S 6R	Reverse: GGA ACC CCT TCT CCA CTT CAG T		52 °C 45 s, 72 °C 50 s); 72 °C 7 min

Table 2. GenBank accession numbers of sequences for species taxa used in the phylogenetic analyses.

Species	COI	ITS–1	18S rDNA	28S rDNA
Recurva postrema	KF308763	–	KF308691	MG45274
Schmidtea mediterranea	JF837062	AF047854	U31085	MG457267
Dugesia adunca	OL505739	OL527659	–	–
D. aenigma	KC006968	KC007043	KF308698	–
D. aethiopica	KY498845	KY498785	KY498822	KY498806
D. afromontana	KY498846	KY498786	KY498823	KY498807
*D. ancoraria1**	OR326966	OR296750	OR198141	OR225689
*D. ancoraria2**	OR326967	OR296751	OR198142	OR225690
*D. ancoraria3**	OR326968	OR296752	OR198143	OR225691
D. arabica	OL410620	OK587374	OK646637	OK491342
D. arcadia	KC006969	KC007047	KF308694	OK491318
D. ariadnae	JN376142	KC007049	OK646636	OK491317
D. aurea	MK712632	MK713027	–	MK712523
D. batuensis	KF907819	KF907816	OK646630	KF907823
D. benazzii	FJ646977, FJ646933	MK713037	OK646628	MK712509
D. bengalensis	–	FJ646897	–	–
D. bifida	KY498851	KY498791	KY498843	KY498813
D. bijuga	MH119630	–	MH113806	–
D. circumcisa	MZ147041	MZ146782	–	–
D. constrictiva	MZ871766	MZ869023	–	–
D. corbata	MK712637	MK713029	–	MK712525
D. cretica	KC006974	KC007055	KF308697	–
D. damoae	KF308768	KC007057	OK646619	OK491310
D. deharvengi	KF907820	KF907817	–	KF907817
D. effusa	KF308780	KC007058	OK646618	OK491311
D. elegans	KC006985	KC007063	KF308695	OK491313
D. etrusca	MK712651	FJ646898	OK646617	OK491312
D. gemmulata	OL632201	–	–	–
D. gibberosa	KY498857	KY498803	KY498842	KY498819
D. gonocephala	FJ646941, FJ646986	FJ646901	DQ666002	DQ665965
D. granosa	OL410634	KY498795	KY498833	KY498816
D. hepta	MK712639	MK713035	OK646612	MK712512
D. ilvana	FJ646989, FJ646944	FJ646903	OK646608	OK491334
D. improvisa	KF308774	KC007065	KF308696	OK491304
D. japonica	AB618487	FJ646906	D83382	DQ665966
D. liguriensis	MK712645	FJ646907	OK646615	OK491353
D. majuscula	MW533425	MW533591	–	–
D. malickyi	KF308750	KC007069	OK646585	OK491294
D. naiadis	KF308757	OK587343	OK646581	OK491293
D. notogaea	FJ646993, FJ646945	FJ646908	KJ599713	KJ599720
D. parasagitta	KF308739	KC007073	OK646577	–
D. pustulata	MH119631	OK587366	MH113807	OK491355
D. ryukyuensis	AB618488	FJ646910	AF050433	DQ665968
D. sagitta	KC007006	KC007085	OK646567	OK491320
D. semiglobosa	MW525210	MW526992	–	–
D. sicula	KF308797	FJ646915	KF308693	DQ665969
D. sigmoides	KY498849	KY498789	KY498827	KY498811
D. sinensis	KP41592	–	–	–
D. subtentaculata	MK712561	MK712995	AF013155	MK712493
D. tubqalis	OM281843	OK587337	OK646555	OK491285
D. tumida	OL505740	OL527709	–	–
D. umbonata	MT176641	MT177211	MT177214	MT177210
D. vilafarrei	MK712648	MK712997	OM281820	MK712511
D. verrucula	MZ147040	MZ146760	–	–

*this study.

Phylogenetic trees were constructed by Maximum Likelihood (ML) and Bayesian Inference (BI) methods. For ML, standard bootstrap analysis with 1,000 replications was performed by IQ-TREE v1.6.2 (Nguyen et al. 2015). BI was performed in MrBayes v3.2.6 (Ronquist et al. 2012) with two simultaneous runs of one cold and three hot chains. Each run for the concatenated dataset was performed for 1,000,000 generations, sampling every 1,000 generations. We checked the resulting parameter file of each run in TRACER v1.7.1 (Rambaut et al. 2018) to ensure that the effective sample size (ESS) values of each parameter were above 200.

Mitochondrial DNA extraction, amplification, sequencing and phylogenetic analysis

After having been starved for three days, the mitochondrial DNA of an asexual specimen of *D. ancoraria* was extracted (due to absence of sexual specimens at that time) using Animal mitochondrial DNA column extraction kit (PCR Grade; BioLebo Technology, Beijing China), followed by amplification of mitochondrial DNA using a REPLI-g Midi Kit (QIAGEN, Hilden, Germany). We compared the COI gene of the three sexual individuals with that of the asexual individual for mitochondrial extraction via megablast and, thus, found that they were perfectly identical. Paired-end sequencing was conducted on the Illumina Hiseq 2500 platform (BGI, Guangzhou, China). The mitogenome sequences were assembled using MitoFinder (Allio et al. 2020). The functional regions of these genes were annotated and verified according to Huang et al. (2022). However, both MITOS (online version: MITOS Web Server (uni-leipzig.de), Bernt et al. 2013) and tRNAscan-SE (Lowe and Chan 2016;) failed to annotate trnT in the mitogenome of *D. ancoraria*. Therefore, trnT was identified manually on the basis of homology comparisons with other species in the family Dugesiidae Ball, 1974. Seven species belonging to Dugesiidae, five to Geoplanidae Stimpson, 1857, and two species belonging to Planariidae Stimpson, 1857 were chosen for the construction of the mitochondrial tree (Table 3). As outgroup taxon we used the maricolan species *Obrimoposthia wandeli* (Hallez, 1906), which is a member of Uteriporidae Diesing, 1862 (Table 3). Multiple sequences alignments (MSA) for protein coding genes (PCGs) and ribosomal genes were carried out using MASCE v2.03, which translates the nucleotides to amino acids before alignment. Hereafter, MSAs were trimmed by Gblocks v0.91b. Substitution saturation tests for each PCG were performed using DAMBE6. Subsequently, SequenceMatrix v1.8 was used to combine the alignments. The best-fit model for each PCG was selected by PartitionFinder2. ML analysis was conducted by IQ-TREE v1.6.2. For BI, MrBayes v3.2.6 was applied with 2,000,000 generations, sampling every 2,000 generations. Gene rearrangement scenarios including reversals, transpositions, reverse transpositions, reversal and tandem-duplication-random-losses (TDRL) among all species were analysed using the software CREx (Bernt et al. 2007) on the CREx web server (http://www.pacosy.informatik.uni-leipzig.de/crex) based on common intervals.

Histology

For the morphological analysis, the flatworms were starved for three days prior to the preparation of histological sections according to procedures described by Song et al. (2020). Briefly, histological sections were made at intervals of 6 μm and were stained with modified Cason's Mallory-Heidenhain stain solution (see Yang et al. 2020). Hereafter, slides were mounted onto glass slides with neutral balsam (Yuanye Biotechnology, Shanghai, China) and sealed with a coverslip. Preparations registered with PLA codes were deposited in the Institute of Zoology, Chinese Academy of Sciences (IZCAS), while histological slides registered with RMNH.VER. codes will be deposited at Naturalis Biodiversity Center, Leiden, The Netherlands.

Abbreviations used in the figures

au: auricle; **bc**: bursal canal; **ca**: common atrium; **cb**: copulatory bursa; **cm**: circular muscle; **d**: diaphragm; **db**: distal bulge; **du**: duct; **e**: eye; **ed**: ejaculatory duct; **esv**: extension seminal vesicle; **go**: gonopore; **hb**: hunchback bump; **ie**: inner epithelium; **lm**: longitudinal muscle; **lod**: left oviduct; **lvd**: left vas deferens; **ma**: male atrium; **od**: oviduct; **oe**: outer epithelium; **ov**: ovary; **pg**: penis glands; **ph**: pharynx; **pp**: penis papilla; **rod**: right oviduct; **rvd**: right vas deferens; **sg**: shell glands; **sv**: seminal vesicle.

Results

Molecular phylogeny

The phylogenetic trees obtained by BI and ML from the concatenated dataset (with the order 18S rDNA–28S rDNA–ITS-1–COI) showed similar topologies and supported nodes (Fig. 2). In this tree, the terminals for *D. ancoraria* grouped together and did not group with any other species of *Dugesia* included in our molecular analysis. It is noteworthy that the new species *D. ancoraria* formed a well-supported clade with *D. notogaea* Sluys & Kawakatsu, 1998 and *D. bengalensis* Kawakatsu, 1972 (Fig. 2, 100% bootstrap [bs] in ML; Suppl. material 1, 1.00 posterior probability [pp] in BI). *Dugesia notogaea* is an Australian species, while *D. bengalensis* inhabits a

Table 3. Species and corresponding GenBank accession numbers of mitochondrial genomes used for mitochondrial analysis.

Species	GenBank	Species	GenBank
Amaga expatria	MT527191	*Obama* sp.	NC026978
Bipalium kewense	NC045216	*Obrimoposthia wandeli*	NC050050
Crenobia alpina	KP208776	*Parakontikia ventrolineata*	MT081960
*Dugesia ancoraria**	OR400685	*Phagocata gracilis*	KP090060
Dugesia japonica	NC016439	*Platydemus manokwari*	MT081580
Dugesia constrictiva	OK078614	*Schmidtea mediterranea*	JX398125
Dugesia ryukyuensis	AB618488		

*this study.

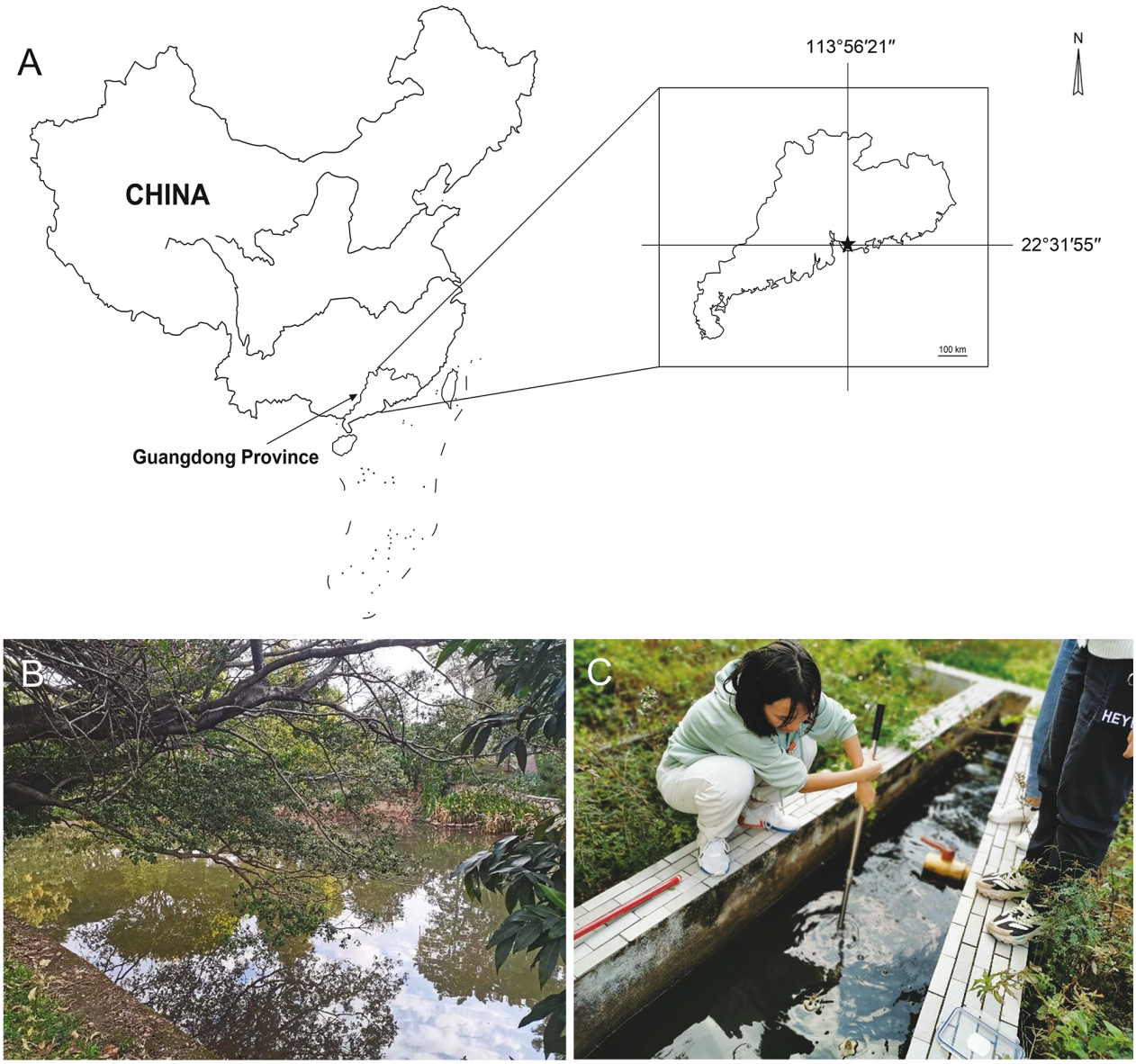

Figure 1. Locality and habitat of *Dugesia ancoraria*. **A.** Sampling locality in Guangdong Province, China; **B, C.** Habitat at sampling locality.

portion of India. As suggested by the high support value (99% bs; 1.00 pp), these three species are closely related and share a sister-group relationship with *D. adunca* Chen & Sluys, 2022 from Guangxi province. Then, these four species are supported as sister to a small clade composed of *D. ryukyuensis* Kawakatsu, 1976 and *D. batuensis* Ball, 1970 (96% bs; 1.00 pp).

Mitochondrial genome

The complete, circular mitochondrial genome of *Dugesia ancoraria* is 17,705 bp in length, and includes 12 of the 13 protein-coding genes of mitochondrial genomes (atp8 was not found), two ribosomal RNA (rRNA) genes, and 22 transfer RNA (tRNA) genes, which are arranged as follows: *cox1-E-nad6-nad5-S2-D-R-cox3-I-Q-K-atp6-V-nad1-W-cox2-P-nad3-A-nad2-M-H-F-rrnS-L1-Y-G-S1-rrnL-L2-T-C-N-cob-nad4l-nad4*. GC content is 23.77%, while a positive GC skew ([G-C]/[G+C] = 0.323) indicated the occurrence of more Gs than Cs (Fig. 3).

Both the ML and BI trees obtained from 12 protein coding genes (PCGs) have highly supported clades, excepting one node with a bootstrap support lower than 70%. Since the topologies of the ML and BI trees are basically identical, we integrated them into one phylogenetic tree. In the integrated tree, *Crenobia alpina* (Dana, 1766) and *Phagocata gracilis* (Haldeman, 1840) together form a clade that shares a sister-group relationship with a clade that is composed of two smaller clades, one comprising land planarians (Geoplanidae) and the other constituted by dugesiid freshwater planarians (Dugesiidae). The latter family forms a well-supported monophyletic group, in which *D. ancoraria* is sister to *D. ryukyuensis* with high support values (100% bs; 1.00 pp) (Fig. 4).

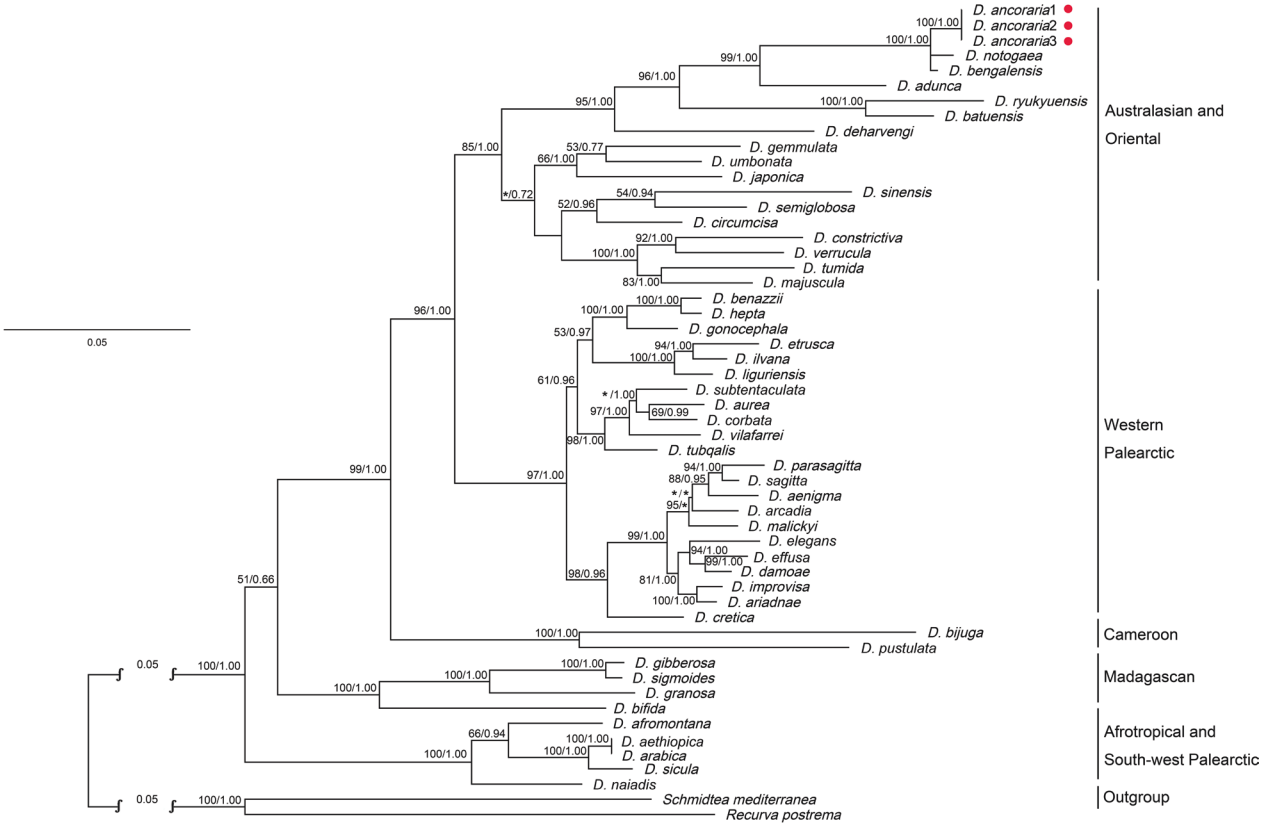

Figure 2. Maximum likelihood phylogenetic tree topology inferred from the concatenated dataset (18S rDNA, ITS-1, 28S rDNA and COI). Numbers at nodes indicate support values (bootstrap/ posterior probability). Asterisks (*) indicate support values lower than 50% bs/0.50 pp, or posterior probability not applicable to this node, because of different topologies of trees generated by BI and ML methods. Scale bar: substitutions per site.

The gene order of rRNAs, PCGs and tRNAs of *D. ancoraria* and other species used in our phylogenetic analysis are shown in Fig. 4. Some tRNAs absent in previous publications, such as those from *Platydemus manokwari* de Beauchamp, 1963 and *Parakontikia ventrolineata* (Dendy, 1892), had been successfully annotated using MITOS (Bernt et al. 2013). Our results show that the orders of PCGs and ribosomal genes are conserved among species belonging to the triclad suborder Continenticola and are arranged as follows: cox1-nad6-nad5-cox3-atp6-nad1-cox2-nad3-nad2-rrnS-rrnL-cob-nad4l-nad4. In contrast, the order of tRNAs is highly variable. Within the cluster of Dugesiidae species, *D. ancoraria* shares an identical gene order with *D. constrictiva*. An analysis of gene order rearrangements with CREx suggests that only one transposition (trnN) occurred from *D. ancoraria* to *D. ryukyuensis* and also one transposition (trnE) from *D. ryukyuensis* to *D. japonica*. Except for a transposition of trnE, a tandem-duplication-random-loss (TDRL) event is required for the transformation from *D. japonica* to *Schmidtea mediterranea* (Benazzi et al., 1975). With respect to the Geoplanidae, *Amaga expatria* Jones & Sterrer, 2005 and *Obama* sp. share the same gene order. Besides a transposition of trnF, a transposition of trnM and trnH linkage is needed to go from *C. alpina* to *Bipalium kewense* Moseley, 1878. Two inverse transpositions, namely trnL2 and trnT, occurred from *Bipalium kewense* to *Obama* sp. and *Amaga expatria*, and from *Obama* sp. to *Platydemus manokwari*, resulting in almost the same gene order shared by *B. kewense* and *P. manokwari*, with the only exception being the position of trnC (Fig. 4).

Systematic account

Order Tricladida Lang, 1884
Suborder Continenticola Carranza, Littlewood, Clough, Ruiz-Trillo, Baguñà & Riutort, 1998
Family Dugesiidae Ball, 1974
Genus *Dugesia* Girard, 1850

***Dugesia ancoraria* Zhu & Wang, sp. nov.**
https://zoobank.org/137337E1-0D52-4288-A3A3-7E8C80241A74

Material examined. *Holotype*: PLA-0251, a narrow artificial canal of Wenshan lake, Shenzhen city, Guangdong Province, China, 22°31'55"N, 113°56'21"E, 10 May 2021, coll. MY Xia and co-workers, sagittal sections on 14 slides.

***Paratypes*:** PLA-0252, ibid., sagittal sections on 12 slides; PLA-0253, ibid., transverse sections on 35 slides; RMNH.VER.21525.1, ibid., sagittal sections on 12 slides.

Habitat. Specimens were collected from a narrow artificial canal running from Wenshan lake (22°31'55"N,

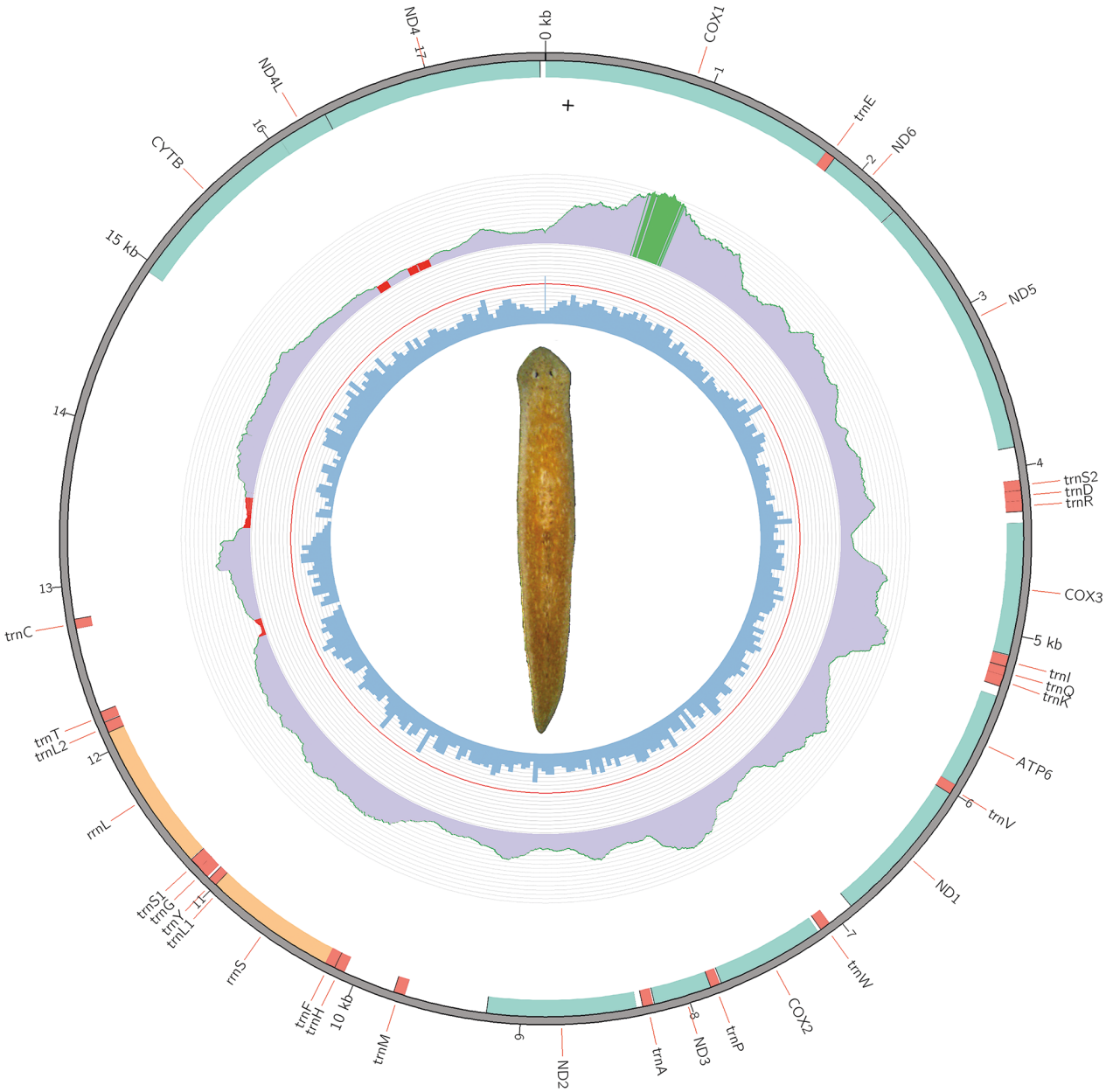

Figure 3. Arrangement of the mitochondrial genome of *Dugesia ancoraria*. Outer circle: annotation of genes, with protein-coding genes, ribosomal RNAs and transfer RNAs represented by cyan, orange, and red, respectively. Intermediate circle: sequencing coverage, with green colour indicating coverage greater than 95% average coverage. Inner circle, with the blue colour indicating GC content and the thin orange circle indicating 50% of GC content. The picture in the middle represents an individual of *D. ancoraria*.

113°56'21"E), which is located in Shenzhen city, Guangdong Province, China (Fig. 1A). The animals were collected from *Cladophora* algae, as well as the stone wall of the canal, which had a water depth of 20–30 cm; water temperature was about 23 °C. Thirty specimens were collected, none of which was sexually mature. However, after six months of rearing under laboratory conditions, about 20 specimens eventually attained sexual maturity.

Diagnosis. *Dugesia ancoraria* is characterised by the following characters: highly asymmetrical penis papilla, provided with a hunchback-like dorsal bump; vasa deferentia opening symmetrically into the mid-lateral section of the more or less ellipsoidal seminal vesicle, which may give rise to a narrow dorsal extension; long and narrow duct connecting seminal vesicle with small diaphragm; ejaculatory duct with a subterminal opening through the ventral surface of the penis papilla; asymmetrical oviducal openings, with the right oviduct opening into a section of the bursal canal that bends ventrally to communicate with the common atrium; the left oviduct opens into the bursal canal at the point where the latter meets the common atrium.

Etymology. The specific epithet is derived from Latin adjective *ancorarius*, of the anchor, and alludes to the penis papilla, which has a hunchback-shape, reminiscent of an anchor, more or less.

Description. Sexualized specimens measured 8.43–9.11 mm in length and 1.13–1.18 mm in width (n = 4;

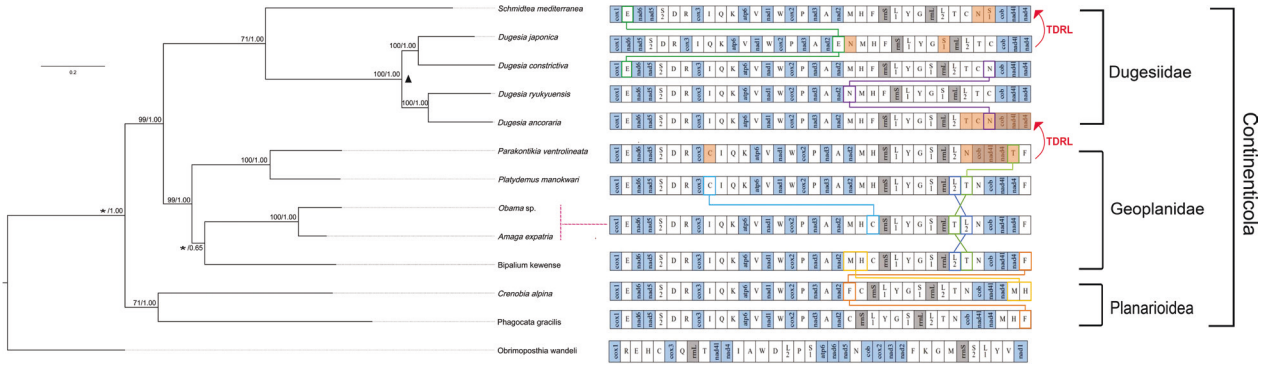

Figure 4. Possible mechanisms of mitochondrial gene rearrangement in Continenticola estimated using CREx, with reference to phylogenetic relationships. On the left-hand side, phylogenetic tree obtained from Maximum likelihood and Bayesian analysis of the concatenated dataset for the protein-coding and rRNA genes within mitochondrial genomes; numbers at nodes indicate support values (pp/bs); Asterisks (*) indicate that bootstrap is not applicable to these nodes because of different topologies of trees generated by BI and ML methods. Pink lines connect species that share the same gene order. On the right-hand side, changes of gene order in mitochondrial genomes in several species of triclad; protein-coding genes in blue, tRNA genes in white, rRNA genes in grey; lines with different colours indicate transpositions of different genes; red lines indicate tandem duplication random loss (TDRL) events between species, while the orange colour indicates where TDRL events occurred.

Fig. 5A, B). Head of low triangular shape with blunt auricles. At the level of the auricles there is a pair of black, bean-shaped eyes, located in pigment-free areas. The distance between the eyes and the lateral body margin is about 0.36–0.46 mm, while the size of the eyecups varies between 210–230 µm. Each eyecup contains numerous retinal cells.

The ground colour of the dorsal surface is brown, dotted with dark brown and white specks; ventral surface much paler than dorsal surface; the body margin is pale (Fig. 5A, B).

The cylindrical pharynx is positioned at about 1/2 of the body and measures about 1/5 of the total body length; the mouth opening is situated at the posterior end of the pharyngeal pocket. The musculature of the pharynx consists of an outer, subepithelial layer of circular muscle, followed by a layer of longitudinal muscle, while the inner musculature is composed of a thick, subepithelial layer of circular muscle, followed by 2–3 layers of longitudinal muscle. The gonopore is situated at about 1/5 of the length of the body, as measured from the posterior body margin (Fig. 5D).

The globular ovaries are located at 1/6 – 1/7 of the distance between the brain and the root of pharynx. From the ovaries, the nucleated oviducts run ventrally in a caudal direction and open separately and asymmetrically into the female reproductive apparatus. Posterior to the gonopore, the right oviduct turns antero-medially and then opens into a section of the bursal canal that bends ventrally to communicate with the common atrium. The left oviduct opens into the bursal canal at the point where the latter meets the common atrium. (Figs 6A, 9B).

A large sac-shaped copulatory bursa is situated immediately behind the pharyngeal pocket and occupies the entire dorso-ventral space; it is lined with a layer of vacuolated, nucleated cells (Figs 6B, 9B). From the bursa, the bursal canal runs in a caudal direction dorso-laterally to the male copulatory apparatus. At the level of the gonopore, the bursal canal curves rather sharply downwards, thus giving rise to a more or less vertically oriented section that opens through the dorsal wall of the common atrium (Figs 6C, 9B).

The bursal canal is lined by a nucleated, columnar glandular epithelium, which is underlain with a layer of longitudinal muscles, followed by 1–4 layers of circular muscles. Along the ventral coat of muscle, ectal reinforcement is present in the form of a single layer of longitudinal muscle running from about the opening of the canal into the common atrium to about 1/3 of the length of the bursal canal (Fig. 9B). Shell glands discharge their cyanophil secretion into the most ventral section of the vertically running portion of the bursal canal, with some glands even discharging into the common atrium (Figs 6B, C, 9B).

The large, near-globular testicular follicles are situated dorsally and extend posteriorly from a short distance behind the brain to well beyond the copulatory apparatus. The male atrium comprises most of the dorso-ventral space of the body (Figs 6A, 9A, B). The large and oval-shaped penis bulb is composed of intermingled longitudinal and circular muscle fibres. The penis papilla has a more or less oblique, postero-ventral orientation or even a vertical orientation, and has a striking shape (Figs 6A, 9A). The papilla is markedly asymmetrical as a result of the course of ejaculatory duct, which opens to the exterior through the postero-ventral wall of the penis papilla. Furthermore, near its root, the papilla has a dorsal bump, which gives it a hunchback appearance (Figs 6A, 9A). The degree of development of this dorsal bump differs between specimens. In the holotype it is highly developed (Fig. 6A), while in paratype PLA-0104 it is somewhat smaller, albeit still well-developed (Fig. 8A), but in paratype PLA-0102 the bump is practically absent (Fig. 7A).

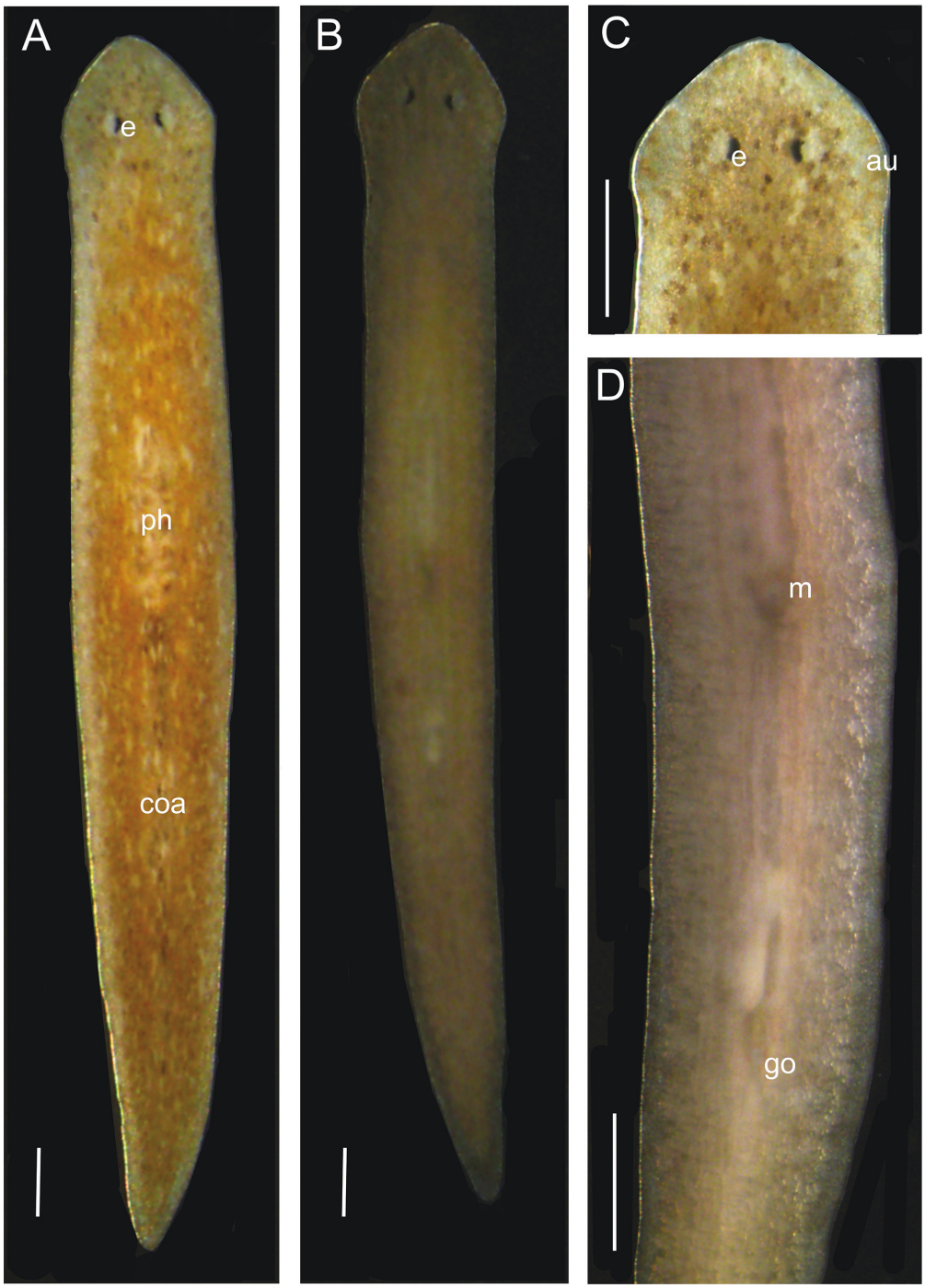

Figure 5. External morphology of *Dugesia ancoraria*. **A.** Living sexual animal in dorsal view; **B.** Living sexual animal in ventral view; **C.** Anterior end, dorsal view; **D.** Ventral view of rear end, showing pharynx, mouth and gonopore. Scale bars: 500 µm.

In addition, the asymmetrical appearance of the penis papilla is enhanced by the fact that the distal portion of the dorsal lip of the papilla gives rise to another bulge, which may be swollen or drawn-out to a greater or lesser extent. In paratype RMNH.VER.21525.1, it is a rather long-drawn bulge (Fig. 8A), whereas in the holotype and paratype PLA-0102 it is more rounded (Fig. 7A). The papilla is covered by a thin, nucleated epithelium, which is underlain with a well-developed, subepithelial layer of circular muscle, followed by a layer of longitudinal muscle at the ventral root.

The vasa deferentia have expanded to form spermiducal vesicles that are packed with sperm. At the level of the penis bulb, the ducts recurve, while decreasing in diameter, run postero-medially for some distance and, thereafter, recurve anteriad before opening separately into the mid-lateral portion of the seminal vesicle (Figs 6A, 9A, B). The vesicle has a more or less ellipsoidal shape, while its dorsal wall may form a narrow extension, which was present in all specimens examined, excepting paratype RMNH.VER.21525.1. The seminal vesicle is lined by a ciliated, nucleated epithelium. A long and narrow duct connects

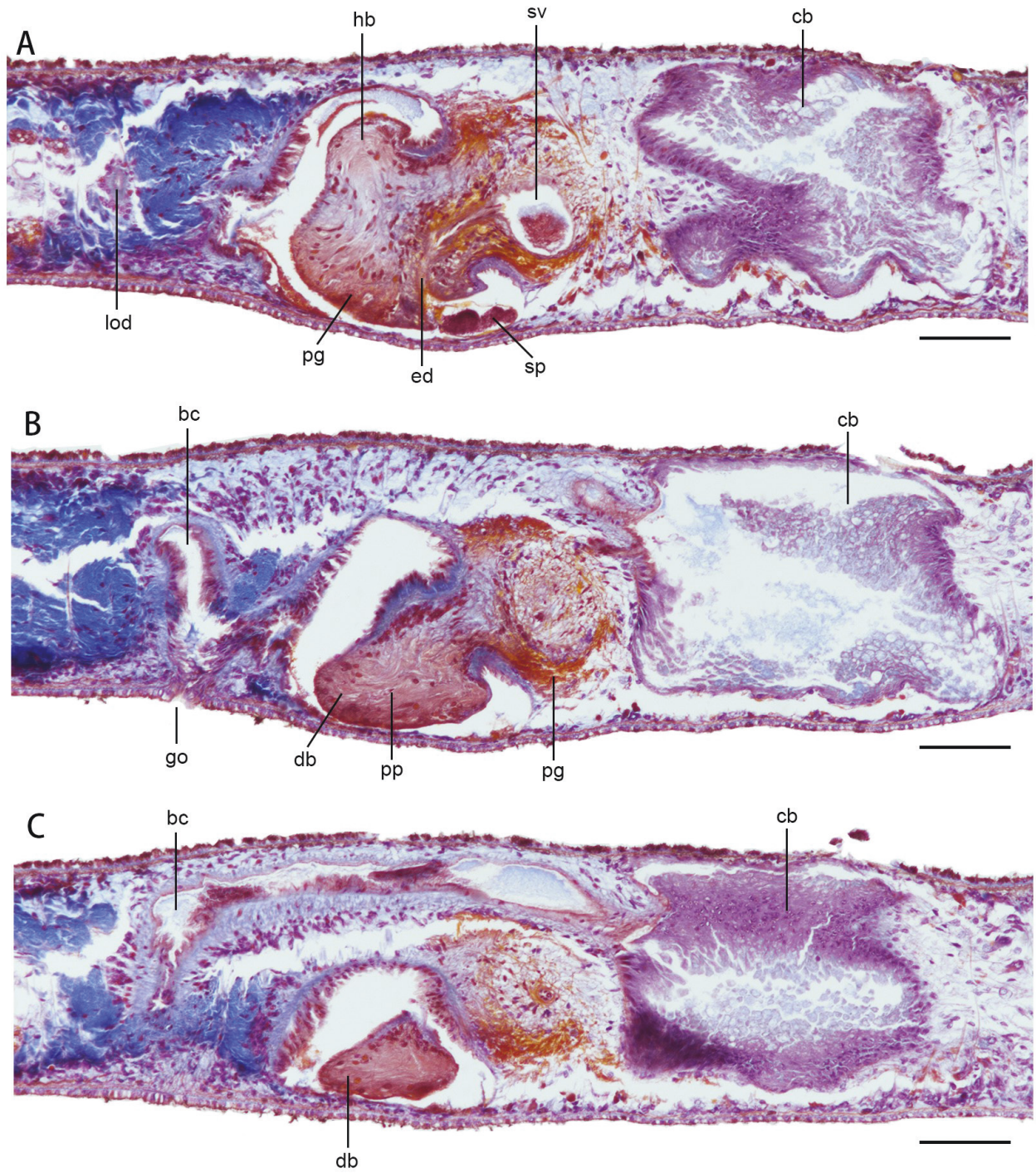

Figure 6. *Dugesia ancoraria*, holotype PLA-0101, sagittal sections, anterior to the right. **A.** Photomicrograph showing copulatory bursa, ejaculatory duct, penis papilla, and seminal vesicle; **B.** Photomicrograph showing copulatory bursa, bursal canal, and gonopore; **C.** Photomicrograph showing copulatory bursa, and bursal canal. Scale bars: 100 µm.

the seminal vesicle with the small diaphragm, which communicates with the ejaculatory duct. The diaphragm receives the abundant secretion of erythrophil penial glands. From the diaphragm, the ejaculatory duct curves strongly postero-ventrally to open subterminally through the ventral epithelium of the penis papilla, thus giving rise to a highly asymmetrical papilla with a large dorsal lip and a small ventral lip (Figs 6A, 9A). Particularly the blunt tip of the dorsal lip of the penis papilla is penetrated by the numerous openings of orange-staining glands.

The male atrium is lined by a nucleated epithelium. The dorsal part of the male atrium is surrounded by a layer of circular muscle, followed by 1–2 layers of longitudinal muscle, while a subepithelial layer of circular muscle, followed by a layer of longitudinal muscle constitutes the musculature on the ventral part of the atrium. The male atrium communicates with the common atrium via a broad opening. The common atrium is lined with a nucleated epithelium, which is underlain by 2–3 layers of circular muscle (Figs 6A, 9).

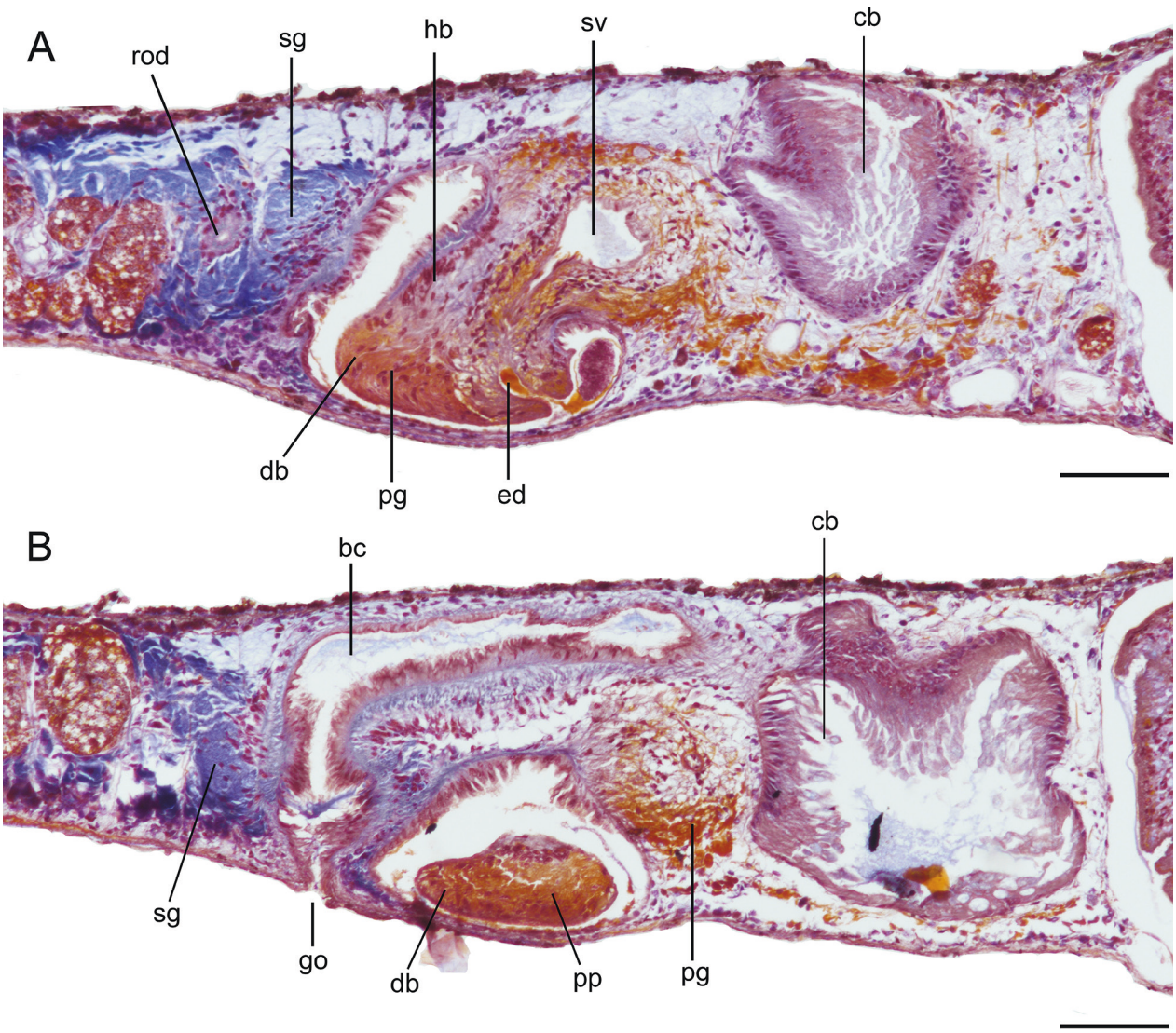

Figure 7. *Dugesia ancoraria*, paratype PLA-0102, sagittal sections. **A.** Photomicrograph showing ejaculatory duct, penis papilla, and seminal vesicle; **B.** Photomicrograph showing copulatory bursa, bursal canal, and gonopore. Scale bars: 100 µm.

Discussion

Molecular phylogeny and biogeography

In our phylogenetic tree (Fig. 2), the terminals for *D. ancoraria* grouped together, while they did not group with any other species of *Dugesia* included in our molecular analysis. Thus, the molecular analysis already suggested that *D. ancoraria* concerns a new species of *Dugesia*, which was supported by the morphological study (see below).

In the phylogenetic trees obtained from the concatenated dataset (Fig. 2), the sister-group relationship between *D. ancoraria* on the one hand and *D. notogaea* and *D. bengalensis* on the other hand is consistent and is supported by high bootstrap values, strongly suggesting that these three species form a monophyletic group. It is noteworthy that *D. ancoraria* from southern China, shares only a distant relationship to other *Dugesia* species from China, including *D. constrictiva*, *D. verrucula*, *D. majuscula*, *D. circumcisa*, *D. semiglobosa*, *D. umbonata*, *D. gemmulata* and *D. tumida*, but is most closely related to *D. notogaea* from Australia and *D. bengalensis* from India. The clade comprising *D. ancoraria*, *D. notogaea* and *D. bengalensis* shares a sister-group relationship with *D. adunca*, then is sister to a small clade comprising *D. ryukyuensis* from Japan and *D. batuensis* from peninsular Malaysia, and then further clusters with *D. deharvengi*, which is basically in agreement with the results of Chen et al. (2022). However, according to Liu et al. (2022), *D. deharvengi* shares a sister-group relationship with *D. notogaea* first, and then clusters with a group comprising *D. ryukyuensis* and *D. batuensis*, which could be due to the absence in the species phylogeny of the COI sequence of *D. bengalensis*. Actually, in the phylogenetic tree generated solely on COI sequences, *D. adunca* shared a sister-group relationship with *D. deharvengi*, albeit with low support, while *D. ryukyuensis* and *D. batuensis* clustered with a clade consisting of *D. majuscula*, *D. verrucula*, *D. constrictiva* and *D. tumida* with very low support (data not shown here), instead of clustering with *D. notogaea* and *D. bengalensis*,

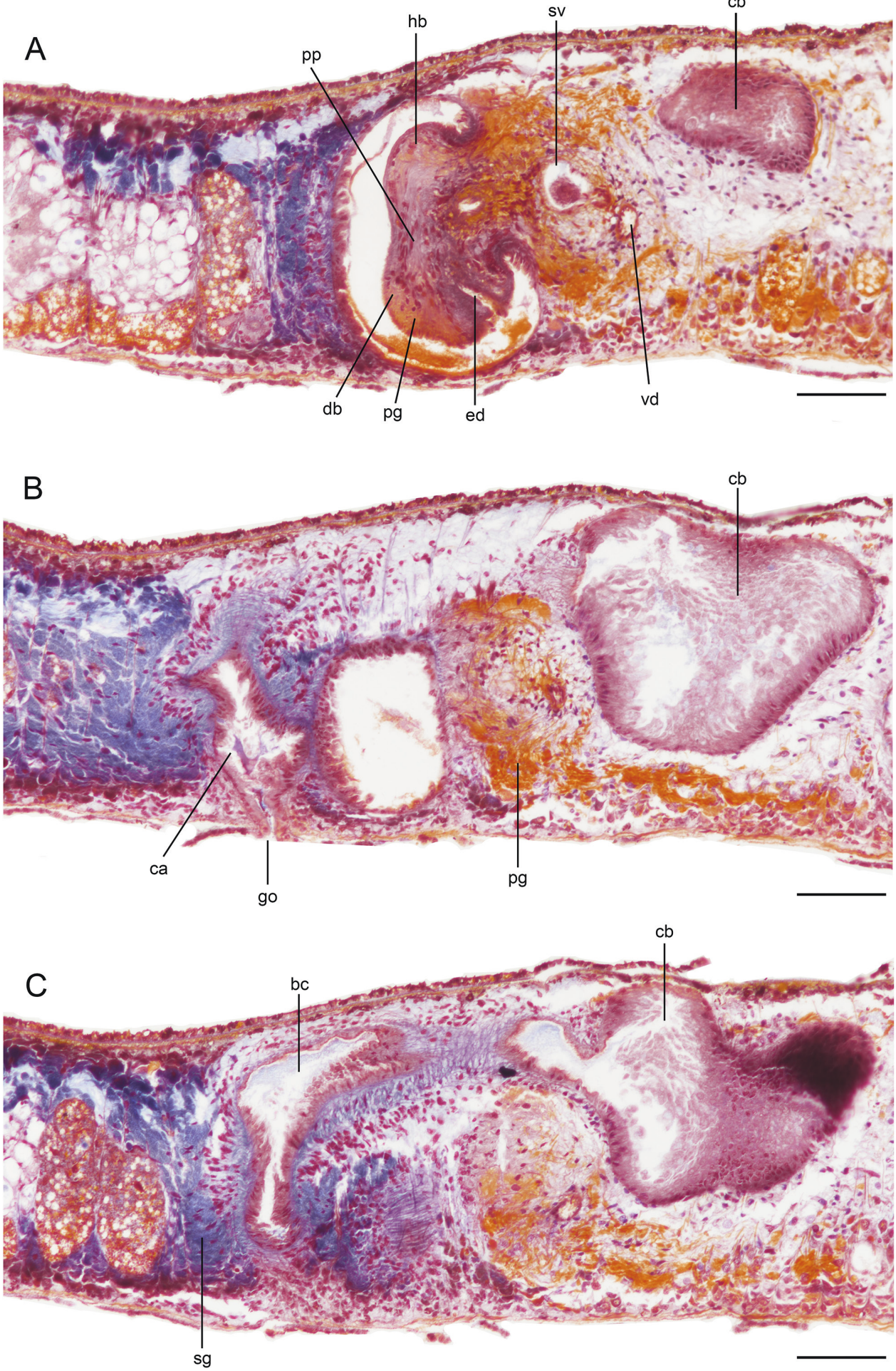

Figure 8. *Dugesia ancoraria*, paratype RMNH.VER.21525.1, sagittal sections. **A.** Photomicrograph showing ejaculatory duct, penis papilla, and seminal vesicle; **B.** Photomicrograph showing copulatory bursa, common atrium, and gonopore; **C.** Photomicrograph showing copulatory bursa, and bursal canal. Scale bars: 100 µm.

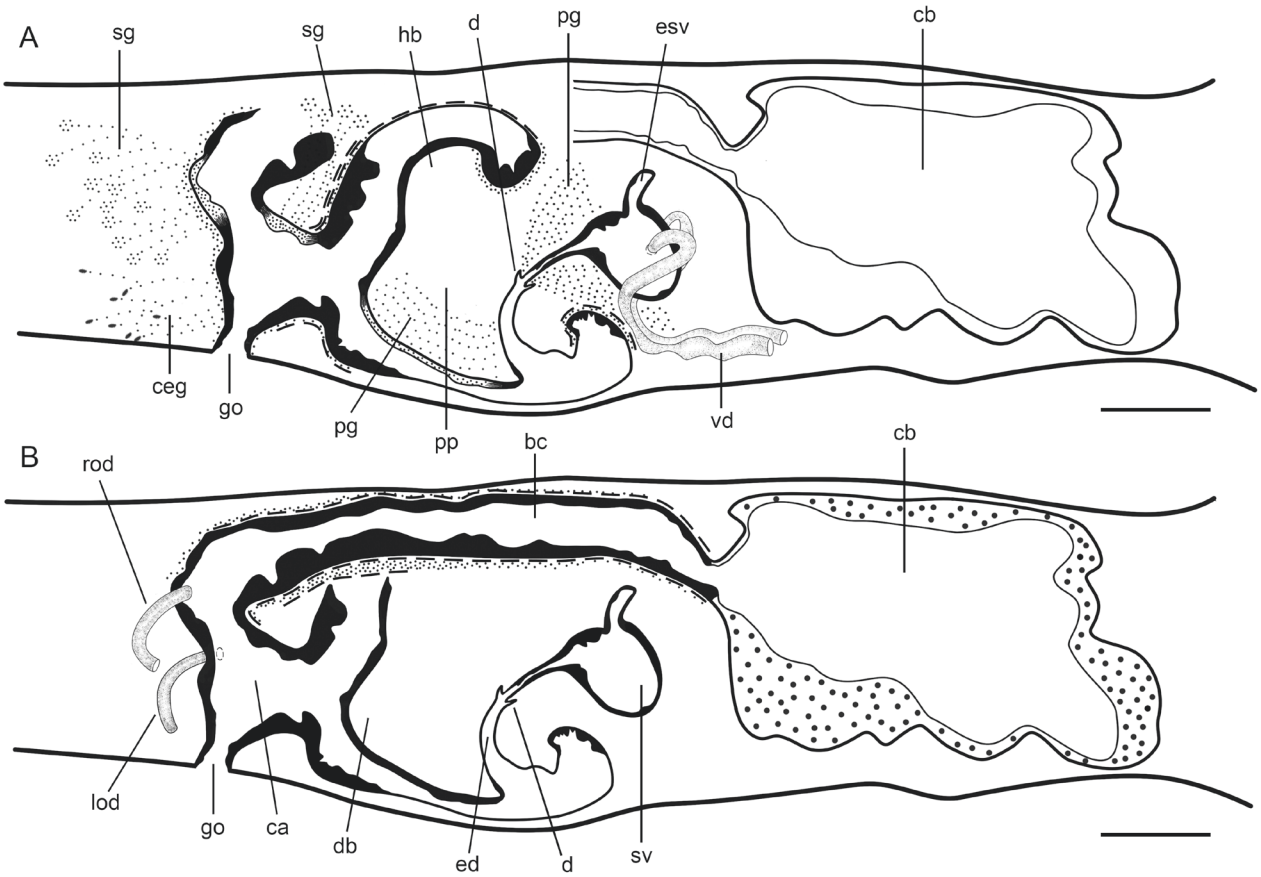

Figure 9. *Dugesia ancoraria*, Sagittal reconstruction of the copulatory apparatus of the holotype. **A.** Male copulatory apparatus; **B.** Female copulatory apparatus. Scale bars: 100 μm.

as in concatenation-based analyses. Furthermore, since different genes may exhibit highly variable rates of evolution, phylogenies inferred from single genes, with only limited evolutionary information, are often inconsistent. Altogether, our results suggested that concatenation-based analyses resulted in more resolved phylogenetic trees.

With respect to the geographical distribution within China of other species of *Dugesia*, in relation to the distribution of *D. ancoraria*, the following should be noted. *Dugesia japonica* has a wide distribution, as it has been reported from the eastern, southern and northern regions of China, while the remaining 11 species are found only in southern China. Among these species, *D. semiglobosa* and *D. majuscula* were documented in Hainan province, *D. circumcisa* and *D. adunca* in Guangxi province, with these two provinces being relatively close to the locality of *D. ancoraria* in Guangdong. *Dugesia tumida* and *D. sinensis* occur also in Guangdong Province, while they share only a very distant relationship with the new species *D. ancoraria*. Other species, like *D. umbonata*, were found in Jiangsu province and *D. gemmulata* in Guizhou. Although these two species are geographically far distant from each other, they share a close relationship.

The close relationship between Chinese *D. ancoraria* and Australian *D. notogaea*, with the latter being the sister-species of Malaysian *D. bengalensis*, is interesting from a historical biogeographic perspective. This pattern of relationships basically agrees with that uncovered by Solà et al. (2022), in which *D. notogaea* also fell into an Asian clade, including specimens from China, Malaysia, Thailand, Japan, and Indonesia. These authors surmised that this pointed to anthropochore dispersal of *Dugesia* from Asia to Australia, as they considered Wallace's Line to indicate an unsurmountable biological barrier for natural arrival of the genus in Australia (see also Ali and Heaney 2022). Excluding unlikely jump dispersal, earlier hypotheses that *Dugesia* naturally spread from Southeast Asia to Australia (Sluys et al. 1998) foundered on the paleogeographical evolution of the Indo-Australian archipelago. According to paleogeographical reconstructions, the river systems of Asia on the one hand and those of Australia/New Guinea on the other hand have never been in contact, not even during the Pleistocene when the sea level was much lower (Sluys et al. 2007). Nevertheless, the distribution of *Dugesia* is repeated by the equally remarkable distribution in Asia and Australasia of portions of the camaenid land snails (Scott 1997; Cuezzo 2003), while the earliest nautiloids from Australia share major characteristics with Asiatic species (Stait and Burrett 1987). Evidently, similarity in these distributional patterns does not imply that they originated during the same period in geological history. Future studies on *Dugesia* from China and the Indo-Australian archipelago would be very interesting, as these may shed light on the biogeographic history of the region.

Annotation of trnT

In our mitogenome analysis, trnT was the only tRNA that could not be automatically annotated by MITOS. However, through translating nucleotides of 12 PCGs to amino acid with Expacy (http://web.expasy.org/translate/), 63 sites of threonine, which is coded by ACN, were found. These results thus support the existence of trnT, which is required for the reading of the triplet of the genetic code (ACN). Therefore, we annotated trnT manually, based on homology comparisons with other species in the family Dugesiidae. Specifically, we aligned the complete mitogenome of *D. ancoraria* with three species belonging to family Dugesiidae, namely *D. japonica*, *D. ryukyuensis* and *D. constrictiva* and found a homologous sequence (60 bp) among these five species, which is particularly conserved at 5' end (AGAA) and 3' end (TTCTT). In addition, the position of trnT of all reported species belonging to Dugesiidae is very conserved and is situated between trnL2 and trnC. Interestingly, the putative trnT in *D. ancoraria* is also located between trnL2 and trnC, providing another line of evidence in support of the annotation. Furthermore, we predicted the secondary structure of trnT manually and presented this through RNAalifold WebServer (http://rna.tbi.univie.ac.at/cgi-bin/RNAWebSuite/RNAfold.cgi) and were surprised to find that the predicted result is not a typical cloverleaf structure with an absence of the DHU stem. By comparing the free energy between the two predicted structures, we found that the free energy with DHU stem (-1.20 kcal/mol) is higher than the one without DHU stem (-4.50 kcal/mol). The absence of the DHU stem in trnT also occurred in several other species of Tricladida, such as *Dugesia japonica*, *D. ryukyuensis*, *Crenobia alpina*, *Obama* sp. and *Schmidtea mediterranea.* (Sakai and Sakaizumi 2012; Solà et al. 2015; Ross et al. 2016). To the best of our knowledge, *P. gracilis* is the only Tricladida species reported to possess trnT with a DHU loop. Therefore, absence of the DHU stem in trnT could be a common phenomenon among species of the Tricladida.

Mitochondrial gene order of suborder Continenticola

In addition, some common features can be discovered in the mitochondrial gene order of the investigated species. Among the five species of Geoplanidae, locations of trnT are variable, in that transpositions of trnT occur in each of two adjacent species in the mitogenome tree, from *B. kewense* to *P. ventrolineata*. Besides, trnF is located at 3' downstream of nad4, with the only exception being *Crenobia alpina*. The gene rearrangement of the maricolan *Obrimoposthia wandeli* differs considerably from species belonging to the suborder Continenticola. Therefore, transformation of gene order in *O. wandeli* to species of the Continenticola may require multiple rearrangements, including reversals, transpositions, and TDRL. Similarly, several TDRL events are required to go from the Geoplanoidea gene order to those of the Dugesiidae species. It is also noteworthy that two species (*D. ancoraria* and *D. constrictiva*) with identical mitochondrial gene order occur in two separate clades. Since gene rearrangements appear to be rare events that may not arise independently in separate lineages (Boore 1999), it is likely that the ancestor of *Dugesia* (indicated by a triangle in Fig. 4) may have had a pattern identical to that of *D. ancoraria* and *D. constrictiva*, implying that in the course of evolutionary history only a transposition of trnE occurred in *D. japonica* as well as transposition of trnN in *D. ryukyuensis*. However, the small number of species for which mitogenomic datasets are currently available, make it presently impossible to test this hypothesis.

Morphological comparisons

A highly asymmetrical penis papilla with both a proximal as well as distal dorsal bumps is the most characteristic feature of *Dugesia ancoraria*. Similar bumps are known only from *D. gibberosa* Stocchino & Sluys, 2017. However, in *D. gibberosa* the penis papilla has a different, ventro-caudal orientation, while its ejaculatory duct opens terminally at the tip of the papilla, in contrast to the subterminal opening in *D. ancoraria*. Moreover, in *D. gibberosa* the bursal canal is surrounded by a very thick layer of circular muscle, while its ectal reinforcement extends more than halfway along the bursal canal. In contrast, the bursal canal musculature in *D. ancoraria* is thinner and the ectal reinforcement weakly developed. Furthermore, *D. ancoraria* and *D. gibberosa* are far removed from each other in the phylogenetic tree (Fig. 2), thus corroborating their separate taxonomic status.

Our molecular analyses, particularly the concatenated dataset, showed that *D. ancoraria* shares a sister-group relationship with Australian *D. notogaea* and Malaysian *D. bengalensis*. Morphologically, all three species have an asymmetrical penis papilla, with the dorsal lip being thicker than ventral lip, and a duct between seminal vesicle and ejaculatory duct. In addition, *D. ancoraria* and *D. notogaea* share the condition in which the oviducts open asymmetrically into the bursal canal. However, there are also clear differences between these three species. For example, in *D. bengalensis* and *D. ancoraria*, the ejaculatory duct has a subterminal opening at the tip of the penis papilla, whereas *D. notogaea* exhibits a terminal opening. In *D. bengalensis* and *D. notogaea*, the vasa deferentia open through the postero-lateral roof of the seminal vesicle, whereas in *D. ancoraria* the ducts open into the mid-lateral portion of the vesicle.

Although *D. gibberosa* is the only other species with two clear dorsal bumps on the penis papilla, there are a number of *Dugesia* species that deserve some comparison with *D. ancoraria*, viz., *D. astrocheta* Marcus, 1958, *D. austroasiatica* Kawakatsu, 1985, and *D. tamilensis* Kawakatsu, 1980. *Dugesia astrocheta* has a clear, proximal hunchback bump on its very asymmetrical penis

papilla, while there is also some indication of a distal bump or bulge (cf. Sluys 2007, fig. 4A). But even when there is indeed such a distal bulge, the species differs in other details from *D. ancoraria*. For example, in *D. ancoraria* there is a relatively long duct interposed between the seminal vesicle and the diaphragm, whereas this duct is virtually absent in *D. astrocheta*. In *D. austroasiatica* there seems to be a rather flexible distal bulge on the dorsal lip of the penis papilla that receives the secretion of glands (cf. Kawakatsu et al. 1986, fig. 3). Apart from the absence of the hunchback, proximal penial bump in *D. austroasiatica*, there are also other differences which signal that it differs from *D. ancoraria*. For example, in the latter the oviducts open asymmetrically into the bursal canal, whereas *D. austroasiatica* has symmetrical oviducal openings. The penis papilla of *D. tamilensis* resembles that of *D. ancoraria* in that it is highly asymmetrical, with the ejaculatory duct opening also at the postero-ventral wall of the papilla, while its dorsal lip is provided also with a distal bulge. However, in this species the oviducts also open symmetrically into the bursal canal, in contrast to the asymmetrical oviducal openings in *D. ancoraria*.

Acknowledgements

This study was supported by grants from Cultivation of Guangdong College Students' Scientific and Technological Innovation ("Climbing Program" Special Funds; grant no. pdjh2023b0449), China Undergraduate Training Program for Innovation and Entrepreneurship (grant no. S202210590072) and the Shenzhen University Innovation Development Fund (grant no. 2021258), as well as grants from the Scientific and Technical Innovation Council of Shenzhen Government (grant nos. jcyj20210324093412035 and kcxfz20201221173404012) and Special Program of Key Sectors in Guangdong Universities (grant no. 2022ZDZX4040). We are grateful to Meng-yu Xia for assistance with sample collection.

References

Ali JR, Heaney LR (2022) Alfred R. Wallace's enduring influence on biogeographical studies of the Indo-Australian archipelago. Journal of Biogeography 50(1): 32–40. https://doi.org/10.1111/jbi.14470

Allio R, Schomaker-Bastos A, Romiguier J, Prosdocimi F, Nabholz B, Delsuc F (2020) MitoFinder: Efficient automated large-scale extraction of mitogenomic data in target enrichment phylogenomics. Molecular Ecology Resources 20(4): 892–905. https://doi.org/10.1111/1755-0998.13160

Bernt M, Merkle D, Ramsch K, Fritzsch G, Perseke M, Bernhard D, Schlegel M, Stadler PF, Middendorf M (2007) CREx. inferring genomic rearrangements based on common intervals. Bioinformatics (Oxford, England) 23(21): 2957–2958. https://doi.org/10.1093/bioinformatics/btm468

Bernt M, Donath A, Juhling F, Externbrink F, Florentz C, Fritzsch G, Putz J, Middendorf M, Stadler PF (2013) MITOS: Improved de novo metazoan mitochondrial genome annotation. Molecular Phylogenetics and Evolution 69(2): 313–319. https://doi.org/10.1016/j.ympev.2012.08.023

Boore JL (1999) Animal mitochondrial genomes. Nucleic Acids Research 27(8): 1767–1780. https://doi.org/10.1093/nar/27.8.1767

Chen GW, Wang L, Wu F, Sun XJ, Dong ZM, Sluys R, Yu F, Yu-wen YQ, Liu DZ (2022) Two new species of *Dugesia* (Platyhelminthes, Tricladida, Dugesiidae) from the subtropical monsoon region in Southern China, with a discussion on reproductive modalities. BMC Zoology 7(25): 1–20. https://doi.org/10.1186/s40850-022-00127-8

Cuezzo MG (2003) Phylogenetic analysis of the *Camaenidae* (Mollusca: Stylommatophora) with special emphasis on the American taxa. Zoological Journal of the Linnean Society 138(4): 449–476. https://doi.org/10.1046/j.1096-3642.2003.00061.x

Huang JJ, Liao YY, Li WX, Li JY, Wang AT, Zhang Y (2022) The complete mitochondrial genome of a marine triclad *Miroplana shenzhensis* (Platyhelminthes, Tricladida, Maricola). Mitochondrial DNA. Part B, Resources 7(6): 927–929. https://doi.org/10.1080/23802359.2022.2079102

Katoh K, Rozewicki J, Yamada KD (2017) Mafft online service: Multiple sequence alignment, interactive sequence choice and visualization. Briefings in Bioinformatics 20(4): 1160–1166. https://doi.org/10.1093/bib/bbx108

Kawakatsu M, Takai M, Oki I, Tamura S, Aoyagi M (1986) A note on an introduced species of freshwater planarian, *Dugesia austroasiatica* Kawakatsu, 1985, collected from culture ponds of *Tirapia mossambica* in Saga City, Kyûshû, Japan (Turbellaria, Tricladida, Paludicola). Bulletin of Fuji Women's College no. 24, ser. II: 87–94.

Lanfear R, Frandsen PB, Wright AM, Senfeld T, Calcott B (2017) PartitionFinder 2: New methods for selecting partitioned models of evolution for molecular and morphological phylogenetic analyses. Molecular Biology and Evolution 34(3): 772–773. https://doi.org/10.1093/molbev/msw260

Li WX, Sluys R, Vila-Farré M, Chen JJ, Yang Y, Li SF, Wang AT (2019) A new continent in the geographic distribution of the genus *Oregoniplana* (Platyhelminthes: Tricladida: Maricola), its rediscovery in South Africa and its molecular phylogenetic position. Zoological Journal of the Linnean Society 187(1): 82–99. https://doi.org/10.1093/zoolinnean/zlz013

Liu Y, Song XY, Sun ZY, Li WX, Sluys R, Li SF, Wang AT (2022) Addition to the known diversity of Chinese freshwater planarians: Integrative description of a new species of *Dugesia* Girard, 1850 (Platyhelminthes, Tricladida, Dugesiidae). Zoosystematics and Evolution 98(2): 233–243. https://doi.org/10.3897/zse.98.83184

Lowe TM, Chan PP (2016) tRNAscan-SE On-line: Search and Contextual Analysis of Transfer RNA Genes. Nucleic Acids Research 44(W1): W54–W57. https://doi.org/10.1093/nar/gkw413

Nguyen LT, Schmidt HA, Haeseler A, Minh BQ (2015) IQ-TREE: A fast and effective stochastic algorithm for estimating maximum-likelihood phylogenies. Molecular Biology and Evolution 32(1): 268–274. https://doi.org/10.1093/molbev/msu300

Rambaut A, Drummond AJ, Xie D, Baele G, Suchard MA (2018) Posterior summarisation in Bayesian phylogenetics using Tracer 1.7. Systematic Biology 67(5): 901–904. https://doi.org/10.1093/sysbio/syy032

Ranwez V, Douzery EJP, Cambon C, Chantret N, Delsuc F (2018) MACSE v2: Toolkit for the alignment of coding sequences accounting for frameshifts and stop codons. Molecular Biology and Evolution 35(10): 2582–2584. https://doi.org/10.1093/molbev/msy159

Ronquist F, Teslenko M, Van der Mark P, Ayres DL, Darling A, Höhna S, Larget B, Liu L, Suchard MA, Huelsenbeck JP (2012) MrBayes 3.2: Efficient Bayesian phylogenetic inference and model choice across a large model space. Systematic Biology 61(3): 539–542. https://doi.org/10.1093/sysbio/sys029

Rosa MT, Oliveira DS, Loreto ELS (2017) Characterization of the first mitochondrial genome of a catenulid flatworm: *Stenostomum leucops* (Platyhelminthes). Journal of Zoological Systematics and Evolutionary Research 55(2): 98–105. https://doi.org/10.1111/jzs.12164

Ross E, Blair D, Guerrero-Hernández C, Alvarado AS (2016) Comparative and transcriptome analyses uncover key aspects of coding and long noncoding RNAs in flatworm mitochondrial genomes. G3 Genes|Genomes|Genetics 6(5): 1191–1200. https://doi.org/10.1534/g3.116.028175

Sakai M, Sakaizumi M (2012) The complete mitochondrial genome of *Dugesia japonica* (Platyhelminthes; Order Tricladida). Zoological Science 29(10): 672–680. https://doi.org/10.2108/zsj.29.672

Scott B (1997) Biogeography of the *Helicoidea* (Mollusca: Gastropoda: Pulmonata): land snails with a Pangean distribution. Journal of Biogeography 24(4): 399–407. https://doi.org/10.1111/j.1365-2699.1997.00106.x

Sluys R (2007) Annotations on freshwater planarians (Platyhelminthes Tricladida Dugesiidae) from the Afrotropical Region. Tropical Zoology 20(2): 229–257.

Sluys R, Riutort M (2018) Planarian diversity and phylogeny. In: Rink JC (Ed.) Planarian Regeneration: Methods and Protocols. Methods in Molecular Biology, vol 1774, Humana Press, Springer Science+Business Media, New York, 1–56. https://doi.org/10.1007/978-1-4939-7802-1_1

Sluys R, Kawakatsu M, Winsor L (1998) The genus *Dugesia* in Australia, with its phylogenetic analysis and historical biogeography (Platyhelminthes, Tricladida, Dugesiidae). Zoologica Scripta 27(4): 273–289. https://doi.org/10.1111/j.1463-6409.1998.tb00461.x

Sluys R, Grant LJ, Blair D (2007) Freshwater planarians from artesian springs in Queensland, Australia (Platyhelminthes, Tricladida, Paludicola). Contributions to Zoology 76(1): 9–19. https://doi.org/10.1163/18759866-07601002

Solà E, Álvarez-Presas M, Frías-López C, Littlewood DTJ, Rozas J, Riutort M (2015) Evolutionary analysis of mitogenomes from parasitic and free-living flatworms. PLoS ONE 10(3): 1–20. https://doi.org/10.1371/journal.pone.0120081

Solà E, Leria L, Stocchino GA, Bagherzadeh R, Balke M, Daniels SR, Harrath AH, Khang TF, Krailas D, Kumar B, Li MH, Maghsoudlou A, Matsumoto M, Naser N, Oben B, Segev O, Thielicke M, Tong X, Zivanovic G, Riutort M (2022) Three dispersal routes out of Africa: The puzzling biogeographical history in freshwater planarians. Journal of Biogeography 49(7): 1219–1233. https://doi.org/10.1111/jbi.14371

Song XY, Li WX, Sluys R, Huang SX, Li SF, Wang AT (2020) A new species of *Dugesia* (Platyhelminthes, Tricladida, Dugesiidae) from China, with an account on the histochemical structure of its major nervous system. Zoosystematics and Evolution 96(2): 431–447. https://doi.org/10.3897/zse.96.52484

Stait B, Burrett C (1987) Biogeography of Australian and Southeast Asian Ordovician nautiloids. In: McKenzie GD (Ed.) Gondwana Six: Stratigraphy, Sedimentology and Paleontology. Washington DC: American Geophysical Union, 21–28. https://doi.org/10.1029/GM041p0021

Steenwyk JL, Buida TJ III, Li Y, Shen XX, Rokas A (2020) ClipKIT: A multiple sequence alignment trimming software for accurate phylogenomic inference. PLoS Biology 18(12): 1–17. https://doi.org/10.1371/journal.pbio.3001007

Talavera G, Castresana J (2007) Improvement of phylogenies after removing divergent and ambiguously aligned blocks from protein sequence alignments. Systematic Biology 56(4): 564–577. https://doi.org/10.1080/10635150701472164

Vaidya G, Lohman DJ, Meier R (2011) SequenceMatrix: Concatenation software for the fast assembly of multi-gene datasets with character set and codon information. Cladistics 27(2): 171–180. https://doi.org/10.1111/j.1096-0031.2010.00329.x

Xia X (2017) DAMBE6: New tools for microbial genomics, phylogenetics, and molecular evolution. The Journal of Heredity 108(4): 431–437. https://doi.org/10.1093/jhered/esx033

Xia X, Lemey P (2009) Assessing substitution saturation with DAMBE. In: Lemey P, Salemi M, Vandamme A (Eds) The phylogenetic handbook: a practical approach to phylogenetic analysis and hypothesis testing. Cambridge University Press, Cambridge, 615–630. https://doi.org/10.1017/CBO9780511819049.022

Xia X, Zheng X, Salemi M, Chen L, Wang Y (2003) An index of substitution saturation and its application. Molecular Phylogenetics and Evolution 26(1): 1–7. https://doi.org/10.1016/S1055-7903(02)00326-3

Yang Y, Li JY, Sluys R, Li WX, Li SF, Wang AT (2020) Unique mating behavior, and reproductive biology of a simultaneous hermaphroditic marine flatworm (Platyhelminthes, Tricladida, Maricola). Invertebrate Biology 139(1): 1–10. https://doi.org/10.1111/ivb.12282

Supplementary material 1

Bayesian inference phylogenetic tree topology

Authors: Ying Zhu, JiaJie Huang, Ronald Sluys, Yi Liu, Ting Sun, An-Tai Wang, Yu Zhang

Data type: docx

Explanation note: Bayesian inference phylogenetic tree topology inferred from the concatenated dataset (18S rDNA, IT-1, 28S DNA and COI). Numbers at nodes indicate support values (posterior probability). Scare bar: substitutions per site.

Link: https://doi.org/10.3897/zse.100.114016.suppl1